



Published in final edited form as:

Chemistry. 2019 August 27; 25(48): 11356–11364. doi:10.1002/chem.201902382.

## The distinct conformational landscapes of 4*S*-substituted prolines that promote an *endo* ring pucker

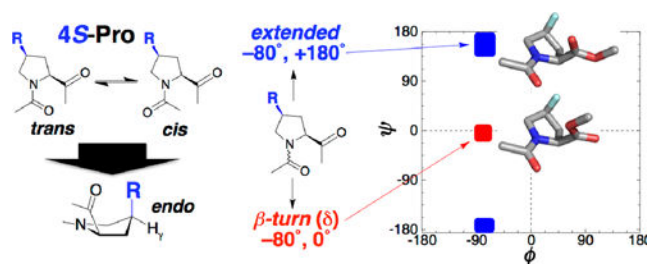
Nicholas V. Costantini, Himal K. Ganguly, Maxwell I. Martin, Nicole A. Wenzell, Glenn P. A. Yap\*, Neal J. Zondlo\*

Department of Chemistry and Biochemistry, University of Delaware, Newark, DE 19716, United States

### Abstract

4-Substitution on proline directly impacts protein main chain conformational preferences. The structural effects of N-acyl substitution and of 4-substitution were examined by NMR spectroscopy and X-ray crystallography on minimal molecules with a proline 4*S*-nitrobenzoate. The effects of N-acyl substitution on conformation were attenuated in the 4*S*-nitrobenzoate context, due to the minimal role of the  $n \rightarrow \pi^*$  interaction in stabilizing extended conformations. By X-ray crystallography, an extended conformation was observed for most molecules. The formyl derivative adopted a  $\delta$  conformation that is observed at the  $i+2$  position of  $\beta$ -turns. Computational analysis indicated that the structures observed crystallographically represent the inherent conformational preferences of 4*S*-substituted prolines with electron-withdrawing 4-position substituents. The divergent conformational preferences of 4*R*- and 4*S*-substituted prolines suggest their wider structure-specific application in molecular design. In particular, the proline *endo* ring pucker favored by 4*S*-substituted prolines uniquely promotes the  $\delta$  conformation ( $(\phi, \psi) \sim (-80^\circ, 0^\circ)$ ) found in  $\beta$ -turns. In contrast to other acyl capping groups, the pivaloyl group strongly promoted *trans* amide bond and polyproline II helix conformation, with a close  $n \rightarrow \pi^*$  interaction in the crystalline state, despite the *endo* ring pucker, suggesting its special capabilities in promoting compact conformations in  $\phi$  due to its strongly electron-donating character.

### Graphical Abstract



\*To whom correspondence should be addressed. zondlo@udel.edu, phone: +1-302-831-0197; gpyap@udel.edu, phone +1-302-831-4441.

Supporting Information Available

Experimental procedures, NMR data on 3–9, NOESY spectra for 7 and 9, X-ray crystallographic data, additional analysis of computational data,  $^1\text{H}$  and  $^{13}\text{C}$  NMR spectra for all new compounds, and coordinates for all geometry-optimized structures.

**Conformational control:** 4*S*-substituted prolines with electron-withdrawing 4-substituents strongly promote the *endo* ring pucker and the  $\delta$  conformation central to  $\beta$ -turns ( $\phi$ ,  $\psi = -80^\circ$ ,  $0^\circ$ ), as determined by X-ray crystallography and calculations. This work suggests their broader application in protein design, medicinal chemistry, and catalysis.

## Introduction

The proline *exo* and *endo* ring puckers have distinct effects on conformational preferences in the protein main chain (torsion angles  $\phi$ ,  $\psi$ , and  $\omega$ ).<sup>[1]</sup> The *exo* ring pucker (C $\gamma$  puckered away from the proline carbonyl; sometimes referred to as the “up” ring pucker) is associated with more compact conformations in  $\phi$  (PPII,  $\alpha$ -helix) (Figure 1).<sup>[1c, 2]</sup> In contrast, the *endo* ring pucker (C $\gamma$  puckered toward the proline carbonyl; “down” ring pucker) is associated with more extended conformations in  $\phi$ . In addition, the *endo* ring pucker is observed to favor the  $\delta$  ( $\phi$ ,  $\psi \sim -90^\circ$ ,  $0^\circ$ ) conformation that is observed at the  $i+2$  position of  $\beta$ -turns.

The  $n \rightarrow \pi^*$  interaction between consecutive carbonyls in proteins stabilizes compact conformations, but only minimally stabilizes more extended conformations.<sup>[3]</sup> In the  $n \rightarrow \pi^*$  interaction of the protein main chain, the lone pair ( $n$ ) of one carbonyl is positioned in a manner that allows orbital overlap with the  $\pi^*$  antibonding orbital of the subsequent carbonyl, with resultant interresidue electron delocalization. This  $n \rightarrow \pi^*$  interaction is most readily identified by  $O_j \dots C_{i+1}$  intercarbonyl distances that are substantially below the 3.22 Å sum of the van der Waals radii of carbon (1.70 Å) and oxygen (1.52 Å). The most favorable  $n \rightarrow \pi^*$  interactions also have an  $O_j C_{i+1} O_{i+1}$  angle close to the Bürgi-Dunitz trajectory ( $O \dots C=O$  angle  $\sim 109^\circ$ ) that allows maximal orbital overlap with the  $\pi^*$  orbital. In addition, in high-resolution structures, pyramidalization can be observed in the acceptor carbonyl, in a manner analogous to early stages of a nucleophilic attack of one carbonyl oxygen on the other carbonyl carbon.<sup>[4]</sup>

We previously demonstrated that the interaction strength of an  $n \rightarrow \pi^*$  interaction could be modulated via the identity of acyl capping groups that change the electronic properties of the donor carbonyl.<sup>[5]</sup> These experiments were conducted using the 4*R*-nitrobenzoate ester of hydroxyproline, which strongly promotes an *exo* ring pucker and thus promotes conformations with a favorable  $n \rightarrow \pi^*$  interaction.<sup>[6]</sup> The observed conformations of 4-substituted prolines are dependent on the stereochemistry and the balance of the electronic *versus* steric effects of the 4-substituent.<sup>[3a, 6b, 7]</sup> The conformational effects of the nitrobenzoate, similar to those of fluorine,<sup>[6a, 6b]</sup> are due to the highly electron-withdrawing nature of the nitrobenzoate group, which leads to its strong preference to be in a pseudo-axial position on the pyrrolidine ring. Effects were observed energetically, via van't Hoff enthalpies of *trans-cis* isomerization equilibria ( $\omega$  torsion angle), as well as crystallographically and computationally, via direct effects on the  $\phi$  and  $\psi$  torsion angles. Thus, electron-donating pivaloyl, *iso*-butyryl, and propionyl groups exhibited conformations ( $\alpha$ -helix, polyproline II helix) with more compact values of  $\phi$  ( $-45^\circ$  to  $-60^\circ$ ) and shorter intercarbonyl distances (as close as 2.68 Å), compared to structures with the acetyl group. In contrast, less electron-donating acyl capping groups (fluoroacetyl, formyl, trifluoroacetyl) exhibited larger intercarbonyl distances (3.05–3.34 Å) and significantly more extended

conformations, despite the presence of the 4*R*-nitrobenzoate. These data indicated that the strength of the  $n \rightarrow \pi^*$  interaction directly impacts the  $\phi$  and  $\psi$  main chain torsion angles, and that the identity of acyl capping groups represents an additional approach to promote defined conformational preferences.

4*R*-Substituted prolines stabilize the polyproline II helix (PPII) conformation present at the Yaa position of collagen, and more generally stabilize the PPII helix via the  $n \rightarrow \pi^*$  interaction.<sup>[3a, 7g, 8]</sup> In contrast, 4*S*-substituted prolines disfavor  $\alpha$ -helix and PPII conformations and adopt more extended conformations, including the Xaa position in collagen, where the  $n \rightarrow \pi^*$  interaction minimally contributes energetically.<sup>[7a, 7b, 7e, 7f, 9]</sup> However, a broader understanding of the conformational preferences of 4*S*-substituted prolines could lead to greater application of these amino acids beyond collagen-mimetic peptides or proteins with *cis*-proline amide bonds.<sup>[7d]</sup> In order to examine this structural landscape, the effects of the acyl capping group were investigated within the context of 4*S*-substituted prolines, which promote conformations that are *not* significantly stabilized by  $n \rightarrow \pi^*$  interactions.

## Results and Discussion

Prolines that are 4*S*-substituted with electron-withdrawing groups promote the *endo* ring pucker.<sup>[7a, 10]</sup> This ring pucker preference is due to a *gauche* effect, in which the 4*S*-substituent is *gauche* to the adjacent C $\beta$ -C $\alpha$  or C $\delta$ -N bonds, which results in the substituent being pseudo-axial on the pyrrolidine ring (Figure 2). This sterically disfavored conformation is preferred because it results in the 4*S*-substituent being *anti*-periplanar to two C-H bonds (C-H $\beta$  and C-H $\delta$ ) (Figure 2b).<sup>[11]</sup> This conformation is stabilized due to hyperconjugation between the  $\sigma_{C-H}$  of the electron-rich C-H bonds and the  $\sigma^*$  antibonding orbital of the C-X bond, which are *syn*-periplanar (eclipsing) to one another, maximizing orbital overlap and electron delocalization. Thus, more electron-withdrawing proline 4-substituents are better electron acceptors both due to more polarized C-X bonds and due to lower energies of the C-X  $\sigma^*$ , resulting in greater stabilization due to hyperconjugation and a greater preference for the *gauche* conformation. Within 4*S*-substituted prolines, the stabilizing effects of hyperconjugation thus lead to a stronger preference for the *endo* ring pucker. Because ring pucker in prolines is associated with main chain conformation, a greater preference for an *endo* ring pucker thus leads to both (1) greater preference for extended or  $\delta$  conformations and (2) a greater likelihood of *cis* proline amide bond.

The effects of 4-substitution on conformation have been extensively examined within collagen model peptides, simple acetylated amino acid methyl esters, and other short model peptides, typically using the  $\omega$  torsion angle ( $K_{trans/cis}$ ) to quantify conformational effects in model compounds and  $T_m$  to quantify conformational effects in collagen model peptides.<sup>[3a, 6a, 6b, 7a, 7b, 7d, 7e, 10a, 12]</sup> In addition, 4-substituted prolines have been examined within a limited number of globular proteins.<sup>[7d, 9b, 13]</sup> In these cases, matching of the stereochemistry of the 4-substituent to the crystallographically observed ring pucker and main chain conformation typically leads to stabilization of the protein structure. In contrast, a mismatch of the proline stereochemistry and the observed conformation at proline leads to

protein destabilization. In addition, 4-substituted prolines have been incorporated in pharmaceuticals and within asymmetric catalysts.<sup>[11b, 14]</sup>

Despite the increasing usage of 4-substituted prolines in medicinal chemistry, protein design, and catalysis, the broad effects of 4-substitution on main chain conformation (particularly  $\phi$  and  $\psi$ ) have not yet been fully appreciated outside of work in collagen model peptides and other examples in protein design. We sought to more generally investigate the conformational landscape of 4-*S*-substituted prolines and to examine the role of capping groups on conformation within 4-*S*-substituted prolines. Therefore, a series of molecules was synthesized based on 4-*S*-hydroxyproline nitrobenzoate methyl ester (Scheme 1). Molecules were synthesized with pivaloyl, *iso*-butyryl, acetyl, trifluoroacetyl, formyl, and Boc N-acyl groups, which represent a range of steric and electronic properties, as well as with the free amine.

All molecules were analyzed by NMR spectroscopy, in order to quantify the effect of the acyl capping group in solution on the equilibrium between *trans* and *cis* amide bonds ( $K_{\text{trans/cis}}$ ) (Table 1). As expected and as has been observed previously in various contexts, most molecules with the 4-*S*-nitrobenzoate diastereomer exhibited a significantly higher population of *cis* amide bond compared to molecules with the 4-*R*-nitrobenzoate. In contrast to prior data with 4-*R*-nitrobenzoates, here, a smaller dependence of  $K_{\text{trans/cis}}$  on donor carbonyl electronic properties was also observed, with the differences in  $K_{\text{trans/cis}}$  more readily explained by steric effects, whereby larger acyl groups sterically disfavor the *cis* amide conformation. The *endo* ring pucker exhibits weaker  $n \rightarrow \pi^*$  interactions, due to the more extended conformation associated with the *endo* ring pucker, consistent with the data herein. In contrast to other molecules, the pivaloyl derivative exhibited exclusively *trans* amide bond by NMR spectroscopy. The size of the pivaloyl group strongly disfavors a *cis* amide bond, which would introduce a large steric clash with the proline carbonyl (Figure 1b).<sup>[15]</sup>

The nitrobenzoate group promotes crystal formation in compounds. Within 4-*R*-substituted hydroxyproline nitrobenzoates, we previously observed that the electronic properties of the acyl capping group dramatically impacted the  $\phi$  and  $\psi$  torsion angles and  $n \rightarrow \pi^*$  interaction intercarbonyl distances, consistent with stronger  $n \rightarrow \pi^*$  interactions with more electron-rich acyl donor carbonyls.<sup>[5b]</sup> Therefore, crystallization was attempted on all compounds, in order to identify the inherent conformational effects of 4-*S*-substituted nitrobenzoates and to examine the ability of acyl donor groups to modulate the conformational preferences.

Single-crystal X-ray structures were solved for compounds **3–9** (Figure 3, Table 2).<sup>[16]</sup> In general, crystal assembly was mediated by aromatic slip-stacking of the nitrobenzoate groups.<sup>[17]</sup> In addition, in all structures, C–H/O interactions with multiple H...O distances significantly (0.2–0.4 Å) below the 2.72 Å sum of the van der Waals radii of H and O were observed at the intermolecular interfaces in the crystals (Figure S26).<sup>[18]</sup> Proline residues exhibit favorable C–H/O interactions in proteins, due in part to the presence of polarized C–H bonds at H $\alpha$  and at both H $\delta$ .<sup>[19]</sup> In 4-substituted prolines, H $\gamma$  is also significantly polarized, rendering these molecules particularly rich in C–H bonds for intermolecular assembly via C–H/O interactions.

These structures were analyzed for their conformational features (Figure 3) and also were compared to the equivalent 4*R*-hydroxyproline nitrobenzoates (Figure 4, Table 2). [5b, 10b, 12b, 20] All proline 4*S*-nitrobenzoates exhibited an *endo* ring pucker, consistent with the strong stereoelectronic effects of the nitrobenzoate group. Indeed, the non-acylated molecules, which lack a donor carbonyl capable of inducing an  $n \rightarrow \pi^*$  interaction, also exhibited an *endo* ring pucker crystallographically, both as the free amine and as the ammonium. Of the other molecules, two had a *trans* amide bond, while four had a *cis* amide bond, consistent with the weak *trans-cis* amide rotameric preference of proline with an *endo* ring pucker.

Among the derivatives with a *cis* amide bond, an extended conformation was observed with the *iso*-butyryl, acetyl, and Boc N-acyl groups. These data are consistent with the significant preference for an extended conformation in proline with an *endo* ring pucker, as well as the weaker  $n \rightarrow \pi^*$  interaction inherent to the *endo* ring pucker.<sup>[1a, 3c]</sup> Notably, the formyl derivative exhibited the  $\delta$  conformation ( $\sim -90^\circ, 0^\circ$ ), which is observed at the *i*-2 position of  $\beta$ -turns.<sup>[21]</sup> Moreover, the conformations observed and the differences between the 4*S*- and the 4*R*- diastereomers were similar to those found in previously reported diastereomeric pairs of 4-substituted prolines (Table 2), suggesting that these results are general. [5b, 10b, 12b, 20]  $\beta$ -Turns are important protein conformations and are common epitopes for protein recognition.<sup>[22]</sup> These crystallographic data suggest the specific utility of 4*S*-substituted prolines to promote  $\beta$ -turn conformations, as well as more extended proline conformations, with potential applications in medicinal chemistry and protein design.<sup>[9b, 23]</sup>

Among molecules with a *trans* amide bond, the trifluoroacetyl derivative exhibited an extended conformation and a longer intercarbonyl distance, consistent with a weak  $n \rightarrow \pi^*$  interaction that is due to both an *endo* ring pucker and an electron-poor donor carbonyl. In contrast, the pivaloyl derivative exhibited a compact value of  $\phi$  ( $-57^\circ$ ) and a close intercarbonyl distance ( $d = 2.76 \text{ \AA}$ ). This conformation is unusually compact for a proline *endo* ring pucker, suggesting that the pivaloyl group promotes particularly favorable  $n \rightarrow \pi^*$  interactions. Indeed, in our prior work on 4*R*-hydroxyproline nitrobenzoates, we observed an unusually close  $n \rightarrow \pi^*$  interaction for the pivaloyl derivative. Collectively, these data indicate that the pivaloyl group is unique in its ability to induce conformations with compact values of  $\phi$ , in addition to its known preference for *trans* amide bonds.

In order to further understand the effects of 4*S*-substitution and acyl capping group on proline conformation, computational investigations were conducted.<sup>[1b, 1c, 2, 5b, 24]</sup> In these calculations, fluorine was used in place of the hydroxyproline nitrobenzoate, due to the similar effects on conformation of both groups<sup>[6a, 6b]</sup> and the substantially greater computational simplicity of fluorine compared to a nitrobenzoate. While the nitrobenzoate group is substantially larger than fluorine, the aromatic ring is rotated away from the proline main chain in the crystal structures herein and observed previously<sup>[5b]</sup>, and thus is not likely to significantly impact the proline conformational preferences. We similarly observed in crystal structures of 4*R*- and 4*S*-iodophenyl hydroxyprolines that the aromatic ring was rotated away from the peptide main chain.<sup>[20a]</sup> Thus, we expect that these computational results should be general for a significant number of 4-substituted prolines with electron-withdrawing 4-substituents. Indeed, in our analysis of the conformational effects of a wide

range of 4-substituted prolines within peptides, we saw broad similarities in the NMR spectra of peptides with the same stereochemistry and similar electronic properties.<sup>[6b]</sup>

Molecules were analyzed with 4*S*-fluoroproline methyl ester as a function of acyl group (pivaloyl, *iso*-butyryl, acetyl, trifluoroacetyl, formyl), amide bond conformation (*trans* versus *cis*), and quadrant of the Ramachandran plot. These calculations were all conducted using the *endo* ring pucker preferred by 4*S*-fluoroproline. These calculations confirmed that, for 4*S*-substituted prolines, the identity of the acyl donor only minimally impacts conformation for most acyl groups, consistent with the weak  $n \rightarrow \pi^*$  interaction associated with the *endo* ring pucker (Table S55). In contrast, the pivaloyl group computationally exhibited a preference for a more compact conformation of  $\phi$  and closer intercarbonyl distances, as had been observed crystallographically. Natural bond orbital (NBO) analysis<sup>[25]</sup> confirmed these conclusions on  $n \rightarrow \pi^*$  interactions, with significantly greater orbital overlap between the donor carbonyl oxygen p-like orbital ( $n_p$ ) and the acceptor carbonyl  $\pi^*$  orbital for the pivaloyl derivative compared to the formyl derivative (Figure 5). Collectively, the data indicate that the pivaloyl group uniquely promotes compact values of  $\phi$  due to particularly favorable  $n \rightarrow \pi^*$  interactions that result from the electron-rich nature of the pivaloyl carbonyl, consistent with the computational results on fluoroproline and the crystallographic results observed for 4*R*- and 4*S*-hydroxyproline nitrobenzoates.

In order to further understand the effects of proline 4-substitution on conformation, computational investigations were conducted on acetyl 4*R*- and 4*S*-fluoroproline methyl ester, as a function of proline amide rotamer (*trans* versus *cis*), ring pucker (*exo* versus *endo*), and quadrant of the Ramachandran plot ( $\alpha_R/\delta$  versus PPII/ $\beta$ ).<sup>[1b, 1c, 2, 5b, 24]</sup> Each combination of diastereomer and conformation was subjected to geometry optimization, and the molecules analyzed for optimized conformation and relative energies. (Figure 6, Table 3). These data confirm the previously observed inherent strong preference of 4*R*-fluoroproline (Flp) for a *trans* amide bond and an *exo* ring pucker, as well as the strong preference of 4*S*-fluoroproline (flp) for an *endo* ring pucker and its weaker preference for a *trans* amide bond. In addition, these calculations are consistent with the previously observed preference of the *exo* ring pucker for more compact conformations, and of the *endo* ring pucker for more extended conformations, independent of fluoroproline stereochemistry. Moreover, these data are consistent with the ability of the fluoroproline to adopt both PPII/ $\beta$  conformations and  $\alpha$ -helical conformations, suggesting broad applications of 4-substituted prolines for conformational control in medicinal chemistry and protein design.

Notably, the fluoroproline diastereomers adopt relatively similar conformations with an *exo* ring pucker, with a compact value of  $\phi$  and similar intercarbonyl  $n \rightarrow \pi^*$  interaction distances observed in either the  $\alpha$ -helical or PPII conformation. In contrast, the observed conformations were different with an *endo* ring pucker. Whereas 4*R*-fluoroproline adopts a somewhat more extended  $\alpha_R$  conformation with an *endo* ring pucker compared to that observed with an *exo* ring pucker, 4*S*-fluoroproline adopts distinct conformations with the *endo* ring pucker. 4*R*-Fluoroproline prefers  $\alpha$ -helical and PPII conformations with an *endo* ring pucker. In contrast, 4*S*-fluoroproline was observed in particular to prefer a more extended or  $\beta$ -turn/ $\delta$  conformation, with significantly more extended values of  $\phi$  ( $\sim -80^\circ$ ), and with  $\psi$  either  $\sim 0^\circ$  or  $+180^\circ$ . These conformational preferences were observed in both

the *trans* and *cis* amide bonds. Combined with the divergent relative energies of these conformations for the 4*R*- and 4*S*-fluoroprolines, these calculations and the analogous structures determined by X-ray crystallography provide strong experimental and computational support that proline diastereomers with electron-withdrawing 4-substituents exhibit distinct conformational landscapes.

4*R*-Substituted prolines prefer more compact conformations with both the *trans* and *cis* amide rotamers, with  $\alpha$ -helical and polyproline helix conformation and compact values of  $\phi$  stabilized. In contrast, 4*S*-substituted prolines exhibit more extended values of  $\phi$  and  $\psi$ . The conformational preferences observed computationally are similar to crystallographic data herein and previously reported for diastereomers of 4*R*- and 4*S*-substituted prolines (Figure 4, Table 2). Notably, this work indicates that 4*S*-substituted prolines strongly promote the  $\delta$  conformation central to  $\beta$ -turns ( $\phi, \psi = -80^\circ, 0^\circ$ ). This conformation (or its mirror image, which would be accessible via the commercially available D-hydroxyproline) is present in type I, I', II, II', and VIa1  $\beta$ -turns, which collectively represent the vast majority of  $\beta$ -turns. [21]  $\beta$ -Turns are central to protein structure and function, and optimized  $\beta$ -turns are widely employed in molecular design. [26]  $\beta$ -Turns are also common recognition elements in proteins, including being a major conformation recognized by GPCRs, and thus are of significant interest in medicinal chemistry. [22] The work herein demonstrates that 4*S*-substituted prolines are unique in their ability to favor this conformation. Collectively, these results suggest the specific consideration of the distinct conformational preferences of 4-substituted prolines as a central component to their application.

## Conclusion

The conformational preferences of proline with an electron-withdrawing 4*S*-substituent were examined by X-ray crystallography, NMR spectroscopy, and computational investigations. A series of derivatives of 4*S*-hydroxyproline nitrobenzoate methyl ester was synthesized with acyl N-capping groups that varied in their steric and electronic properties. All molecules exhibited an *endo* ring pucker crystallographically. For most acyl derivatives, only a modest preference for a *trans* versus *cis* amide bond was observed, with minimal evidence of a significant  $n \rightarrow \pi^*$  interaction with the *endo* ring pucker. In this context, steric effects were the major determinant of *trans* versus *cis* amide bond. More extended conformations were observed for 4*S*-substitution than were observed with 4*R*-substitution, with  $\phi \sim -80^\circ$  and  $\psi \sim 0^\circ$  or  $180^\circ$  seen crystallographically for the 4*S*-hydroxyproline nitrobenzoates and computationally for 4*S*-fluoroprolines. The  $\delta$  conformation adopted in  $\beta$ -turns in particular was observed both crystallographically and computationally as a preferred conformation of 4*S*-substituted prolines with an *endo* ring pucker. Given the importance of  $\beta$ -turns in protein structure and as recognition motifs in biology and medicinal chemistry, these results suggest the specific application of 4*S*-substituted prolines in these contexts. Direct comparison of the structures of the 4*R*- and 4*S*- diastereomers of a series of derivatives emphasizes the distinct conformational preferences of the 4-substituted prolines. The 4*R*-substituted prolines prefer an *exo* ring pucker and promote compact conformations that are stabilized by  $n \rightarrow \pi^*$  interactions. In contrast, the 4*S*-substituted prolines prefer an *endo* ring pucker and promote more extended conformations in  $\phi$  and/or  $\psi$ . Notably, even in the 4*S*-hydroxyproline nitrobenzoate, the pivaloyl group uniquely induced a compact value of  $\phi$  and a close  $n \rightarrow \pi^*$

interaction, with the molecule in a polyproline II helix conformation. These results suggest a special ability of the pivaloyl group to promote the  $n \rightarrow \pi^*$  interaction and polyproline II helix.

## Experimental

### Synthesis.

All compounds were synthesized using variations on previously described methods. Details are in the Supporting Information.

### NMR spectroscopy.

Compounds **3–9** were analyzed by NMR spectroscopy in  $\text{CDCl}_3$ , with 32,768 data points and a relaxation delay of 2.0 s. The populations of the *trans* and *cis* rotamers were quantified via the  $\text{H}_\alpha$  resonances using baseline-corrected spectra. NOESY experiments were conducted on **7** and **9** to confirm the assignments of the *trans* and *cis* amide rotamers. Additional details, expansions of key spectral regions, and NOESY data are in the Supporting Information.

### X-ray crystallography.

Compounds crystallized from solutions in ethyl acetate or from solutions of ethyl acetate in hexanes. Structures were determined by X-ray diffraction and have been deposited in the Cambridge Structural Database under CCDC 1914568–1914575.<sup>[16]</sup> Additional details are in the Supporting Information.

### Computational chemistry.

Calculations were conducted with Gaussian09.<sup>[27]</sup> Natural bond orbital (NBO) analysis<sup>[25]</sup> was conducted using the implementation of NBO within Gaussian. Visualization was conducted with GaussView 5, using isovalues of 0.02 for molecular orbitals. Geometry optimization was conducted using the M06–2X DFT method.<sup>[28]</sup> Initial models were generated using proline derivatives with each combination of the following conformational pairs: *trans* or *cis* amide bonds; *exo* or *endo* ring pucker; and combinations of  $\phi$  and  $\psi$  corresponding to  $\alpha$ -helix or polyproline II helix. Models were initially optimized using the 6–311++G(d,p) basis set.<sup>[29]</sup> These initial models were subsequently optimized using the 6–311++G(2d,2p), then 6–311++G(3d,3p), basis sets, using implicit water solvation (IEFPCM continuum polarization model). These models were subjected to frequency analysis. If necessary, geometry optimization was continued until there were zero imaginary frequencies. All final models had zero imaginary frequencies.

## Supplementary Material

Refer to Web version on PubMed Central for supplementary material.

## Acknowledgements

We thank NSF (CHE-1412978) for funding. We thank the David A. Plastino Undergraduate Research Scholars Program for support for NAW. Instrumentation support was provided by NIH (GM110758) and NSF



(CHE-1229234). Molecular graphics in Figure 4 were created using UCSF Chimera, developed by the Resource for Biocomputing, Visualization, and Informatics at the University of California, San Francisco, with support from NIH P41-GM103311.

## References

- [1]. aMilner-White EJ, Bell LH, Maccallum PH, *J. Mol. Biol.* 1992, 228, 725–734; [PubMed: 1469711] bVitagliano L, Berisio R, Mastrangelo A, Mazarella L, Zagari A, *Protein Sci.* 2001, 10, 2627–2632; [PubMed: 11714932] cKang YK, Choi HY, *Biophys. Chem.* 2004, 111, 135–142; [PubMed: 15381311] dHo BK, Coutias EA, Seok C, Dill KA, *Protein Sci.* 2005, 14, 1011–1018. [PubMed: 15772308]
- [2]. Aliev AE, Bhandal S, Courtier-Murias D, *J. Phys. Chem. A* 2009, 113, 10858–10865. [PubMed: 19757781]
- [3]. aBretscher LE, Jenkins CL, Taylor KM, DeRider ML, Raines RT, *J. Am. Chem. Soc.* 2001, 123, 777–778; [PubMed: 11456609] bBartlett GJ, Choudhary A, Raines RT, Woolfson DN, *Nat. Chem. Biol.* 2010, 6, 615–620; [PubMed: 20622857] cNewberry RW, Raines RT, *Acc. Chem. Res.* 2017, 50, 1838–1846; [PubMed: 28735540] dSingh SK, Das A, *Phys. Chem. Chem. Phys.* 2015, 17, 9596–9612; [PubMed: 25776003] eSingh SK, Mishra KK, Sharma N, Das A, *Angew. Chem., Int. Ed.* 2016, 55, 7801–7805.
- [4]. Choudhary A, Newberry RW, Raines RT, *Org. Lett.* 2014, 16, 3421–3423. [PubMed: 24926562]
- [5]. aNewberry RW, VanVeller B, Guzei IA, Raines RT, *J. Am. Chem. Soc.* 2013, 135, 7843–7846; [PubMed: 23663100] bWenzell NA, Ganguly HK, Bhatt MR, Yap GPA, Zondlo NJ, *ChemBioChem* 2019, 20, 963–967. [PubMed: 30548564]
- [6]. aThomas KM, Naduthambi D, Tririya G, Zondlo NJ, *Org. Lett.* 2005, 7, 2397–2400; [PubMed: 15932207] bPandey AK, Naduthambi D, Thomas KM, Zondlo NJ, *J. Am. Chem. Soc.* 2013, 135, 4333–4363; [PubMed: 23402492] cPandey AK, Yap GPA, Zondlo NJ, *J. Org. Chem.* 2014, 79, 4174–4179. [PubMed: 24720652]
- [7]. aHodges JA, Raines RT, *J. Am. Chem. Soc.* 2003, 125, 9262–9263; [PubMed: 12889933] bHorng JC, Raines RT, *Protein Sci.* 2006, 15, 74–83; [PubMed: 16373476] cShoulders MD, Hodges JA, Raines RT, *J. Am. Chem. Soc.* 2006, 128, 8112–8113; [PubMed: 16787056] dRenner C, Alefelder S, Bae JH, Budisa N, Huber R, Moroder L, *Angew. Chem., Int. Ed.* 2001, 40, 923–925; eUmashankara M, Babu IR, Ganesh KN, *Chem. Commun.* 2003, 2606–2607; fKim W, Hardcastle KI, Conticello VP, *Angew. Chem., Int. Ed.* 2006, 45, 8141–8145; gSonntag LS, Schweizer S, Ochsenfeld C, Wennemers H, *J. Am. Chem. Soc.* 2006, 128, 14697–14703. [PubMed: 17090057]
- [8]. aBabu IR, Ganesh KN, *J. Am. Chem. Soc.* 2001, 123, 2079–2080; [PubMed: 11456840] bPersikov AV, Ramshaw JAM, Kirkpatrick A, Brodsky B, *J. Am. Chem. Soc.* 2003, 125, 11500–11501. [PubMed: 13129344]
- [9]. aDoi M, Nishi Y, Uchiyama S, Nishiuchi Y, Nakazawa T, Ohkubo T, Kobayashi Y, *J. Am. Chem. Soc.* 2003, 125, 9922–9923; [PubMed: 12914445] bKim W, McMillan RA, Snyder JP, Conticello VP, *J. Am. Chem. Soc.* 2005, 127, 18121–18132; [PubMed: 16366565] cLin Y-J, Horng J-C, *Amino Acids* 2014, 46, 2317–2324; [PubMed: 24947982] dTressler CM, Zondlo NJ, *J. Org. Chem.* 2014, 79, 5880–5886. [PubMed: 24870929]
- [10]. aErdmann RS, Kumin M, Wennemers H, *Chimia* 2009, 63, 197–200; bShoulders MD, Kotch FW, Choudhary A, Guzei IA, Raines RT, *J. Am. Chem. Soc.* 2010, 132, 10857–10865. [PubMed: 20681719]
- [11]. aThiehoff C, Rey YP, Gilmour R, *Isr. J. Chem.* 2017, 57, 92–100; bAufiero M, Gilmour R, *Acc. Chem. Res.* 2018, 51, 1701–1710. [PubMed: 29894155]
- [12]. aJenkins CL, McCloskey AI, Guzei IA, Eberhardt ES, Raines RT, *Biopolymers* 2005, 80, 1–8; [PubMed: 15558658] bKotch FW, Guzei IA, Raines RT, *J. Am. Chem. Soc.* 2008, 130, 2952–2953; [PubMed: 18271593] cTaylor CM, Hardré R, Edwards PJB, Park JH, *Org. Lett.* 2003, 5, 4413–4416; [PubMed: 14602013] dTaylor CM, Hardre R, Edwards PJB, *J. Org. Chem.* 2005, 70, 1306–1315; [PubMed: 15704965] eChiang YC, Lin YJ, Horng JC, *Protein Sci.* 2009, 18, 1967–1977; [PubMed: 19609932] fKubyshevskii V, Pridma, Budisa N, *New J. Chem.* 2018, 42.

- [13]. aNaduthambi D, Zondlo NJ, *J. Am. Chem. Soc* 2006, 128, 12430–12431; [PubMed: 16984189] bZheng T-Y, Lin Y-J, Horng J-C, *Biochemistry* 2010, 49, 4255–4263; [PubMed: 20405858] cHolzberger B, Marx A, *J. Am. Chem. Soc* 2010, 132, 15708–15713; [PubMed: 20961065] dHolzberger B, Obeid S, Welte W, Diederichs K, Marx A, *Chem. Sci* 2012, 3; eTang HC, Lin YJ, Horng JC, *Proteins Struct. Funct. Bioinform* 2014, 82, 67–76; fCrespo MD, Rubini M, *PLoS One* 2011, 6, e19425; [PubMed: 21625626] gRoderer D, Glockshuber R, Rubini M, *ChemBioChem* 2015, 16, 2162–2166. [PubMed: 26382254]
- [14]. aChandler CL, List B, *J. Am. Chem. Soc* 2008, 130, 6737–6739; [PubMed: 18454521] bMyers EL, Palte MJ, Raines RT, *J. Org. Chem* 2019, 84, 1247–1256. [PubMed: 30602119]
- [15]. aLiang G-B, Rito, Gellman SH, *Biopolymers* 1992, 32, 293–301; [PubMed: 1581548] bRai R, Aravinda S, Kanagarajadurai K, Raghothama S, Shamala N, Balaram P, *J. Am. Chem. Soc* 2006, 128, 7916–7928; [PubMed: 16771506] cReddy DN, Prabhakaran EN, *Biopolymers* 2014, 101, 66–77; [PubMed: 23653336] dMeng HY, Thomas KM, Lee AE, Zondlo NJ, *Biopolymers (Peptide Sci.)* 2006, 84, 192–204.
- [16]. Groom CR, Bruno IJ, Lightfoot MP, Ward SC, *Acta Cryst.* 2016, B72, 171–179.
- [17]. aHunter CA, Sanders JKM, *J. Am. Chem. Soc* 1990, 112, 5525–5534; bSalonen LM, Ellermann M, Diederich F, *Angew. Chem., Int. Ed* 2011, 50, 4808–4842.
- [18]. aDesiraju GR, *Acc. Chem. Res* 1996, 29, 441–449; [PubMed: 23618410] bGu YL, Kar T, Scheiner, *J. Am. Chem. Soc* 1999, 121, 9411–9422; cJones CR, Baruah PK, Thompson AL, Scheiner S, Smith MD, *J. Am. Chem. Soc* 2012, 134, 12064–12071; [PubMed: 22789294] dAdhikari U, Scheiner S, *J. Phys. Chem. A* 2013, 117, 10551–10562; [PubMed: 24028630] eSteiner T, *Angew. Chem., Int. Ed* 2002, 41, 48–76.
- [19]. aHorowitz S, Trievel RC, *J. Biol. Chem* 2012, 287, 41576–41582; [PubMed: 23048026] bSenes A, Ubarretxena-Belandia I, Engelman DM, *Proc. Natl. Acad. Sci. U.S.A.* 2001, 98, 9056–9061; [PubMed: 11481472] cBella J, Berman HM, *J. Mol. Biol* 1996, 264, 734–742. [PubMed: 8980682]
- [20]. aForbes CR, Pandey AK, Ganguly HK, Yap GPA, Zondlo NJ, *Org. Biomol. Chem* 2016, 14, 2327–2346; [PubMed: 26806113] bPanasik N, Eberhardt ES, Edison AS, Powell DR, Raines RT, *Int. J. Peptide Protein Res.* 1994, 44, 262–269; [PubMed: 7822103] cWoinska M, Grabowsky S, Dominiak PM, Wozniak K, Jayatilaka D, *Sci. Adv* 2016, 2, e1600192; [PubMed: 27386545] dClegg W, Deboves HJC, Elsegood MRJ, *Acta. Cryst* 2003, E59, o1987–01989.
- [21]. Hutchinson EG, Thornton JM, *Protein Sci.* 1994, 3, 2207–2216. [PubMed: 7756980]
- [22]. Tyndall JDA, Pfeiffer B, Abbenante G, Fairlie DP, *Chem. Rev* 2005, 105, 793–826. [PubMed: 15755077]
- [23]. Quancard J, Karoyan P, Lequin O, Wenger E, Aubry A, Lavielle S, Chassaing G, *Tetrahedron Lett.* 2004, 45, 623–625.
- [24]. DeRider ML, Wilkens SJ, Waddell MJ, Bretscher LE, Weinhold F, Raines RT, Markley JL, *J. Am. Chem. Soc* 2002, 124, 2497–2505. [PubMed: 11890798]
- [25]. Glendening CR, Landis CR, Weinhold F, *WIREs Comput. Mol. Sci* 2012, 2, 1–42.
- [26]. aHaque TS, Little JC, Gellman SH, *J. Am. Chem. Soc* 1994, 116, 4105–4106; bStruthers MD, Cheng RP, Imperiali B, *Science* 1996, 271, 342–345; [PubMed: 8553067] cStanger HE, Gellman SH, *J. Am. Chem. Soc* 1998, 120, 4236–4237; dTatko CD, Waters ML, *J. Am. Chem. Soc* 2002, 124, 9372–9373; [PubMed: 12167022] eSchneider JP, Pochan DJ, Ozbas B, Rajagopal K, Pakstis L, Kretsinger J, *J. Am. Chem. Soc* 2002, 124, 15030–15037. [PubMed: 12475347]
- [27]. Frisch MJ, Trucks GW, Schlegel HB, Scuseria GE, Robb MA, Cheeseman JR, Scalmani G, Barone V, Mennucci B, Petersson GA, Nakatsuji H, Caricato M, Li X, Hratchian HP, Izmaylov AF, Bloino J, Zheng G, Sonnenberg JL, Hada M, Ehara M, Toyota K, Fukuda R, Hasegawa J, Ishida M, Nakajima T, Honda Y, Kitao O, Nakai H, Vreven T, Montgomery J, J. A., Peralta JE, Ogliaro F, Bearpark M, Heyd JJ, Brothers E, Kudin KN, Staroverov VN, Keith T, Kobayashi R, Normand J, Raghavachari K, Rendell A, Burant JC, Iyengar SS, Tomasi J, Cossi M, Rega N, Millam JM, Klene M, Knox JE, Cross JB, Bakken V, Adamo C, Jaramillo J, Gomperts R, Stratmann RE, Yazyev O, Austin AJ, Cammi R, Pomelli C, Ochterski JW, Martin RL, Morokuma K, Zakrzewski VG, Voth GA, Salvador P, Dannenberg JJ, Dapprich S, Daniels AD, Farkas O, Foresman JB, Ortiz JV, Cioslowski J, Fox DJ, Gaussian, Inc, Wallingford, CT, 2013.
- [28]. Zhao Y, Truhlar DG, *Theor. Chem. Act* 2008, 120, 215–241.

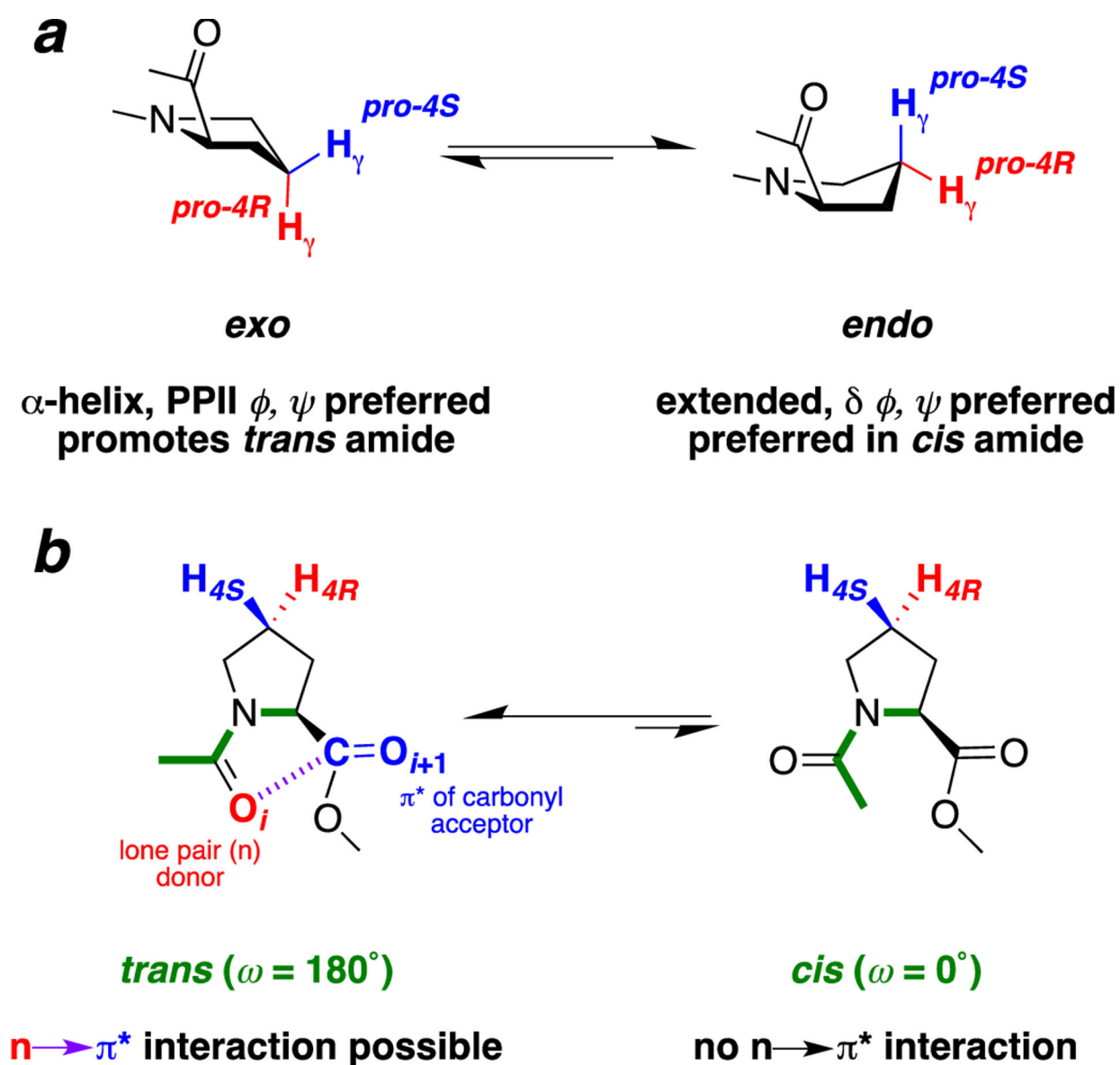
- [29]. Raghavachari K, Binkley JS, Seeger R, Pople JA, J. Chem. Phys 1980, 72, 650–654.
- [30]. Pettersen EF, Goddard TD, Huang CC, Couch GS, Greenblatt DM, Meng EC, Ferrin TE, J. Comput. Chem 2004, 25, 1605–1612. [PubMed: 15264254]

Author Manuscript

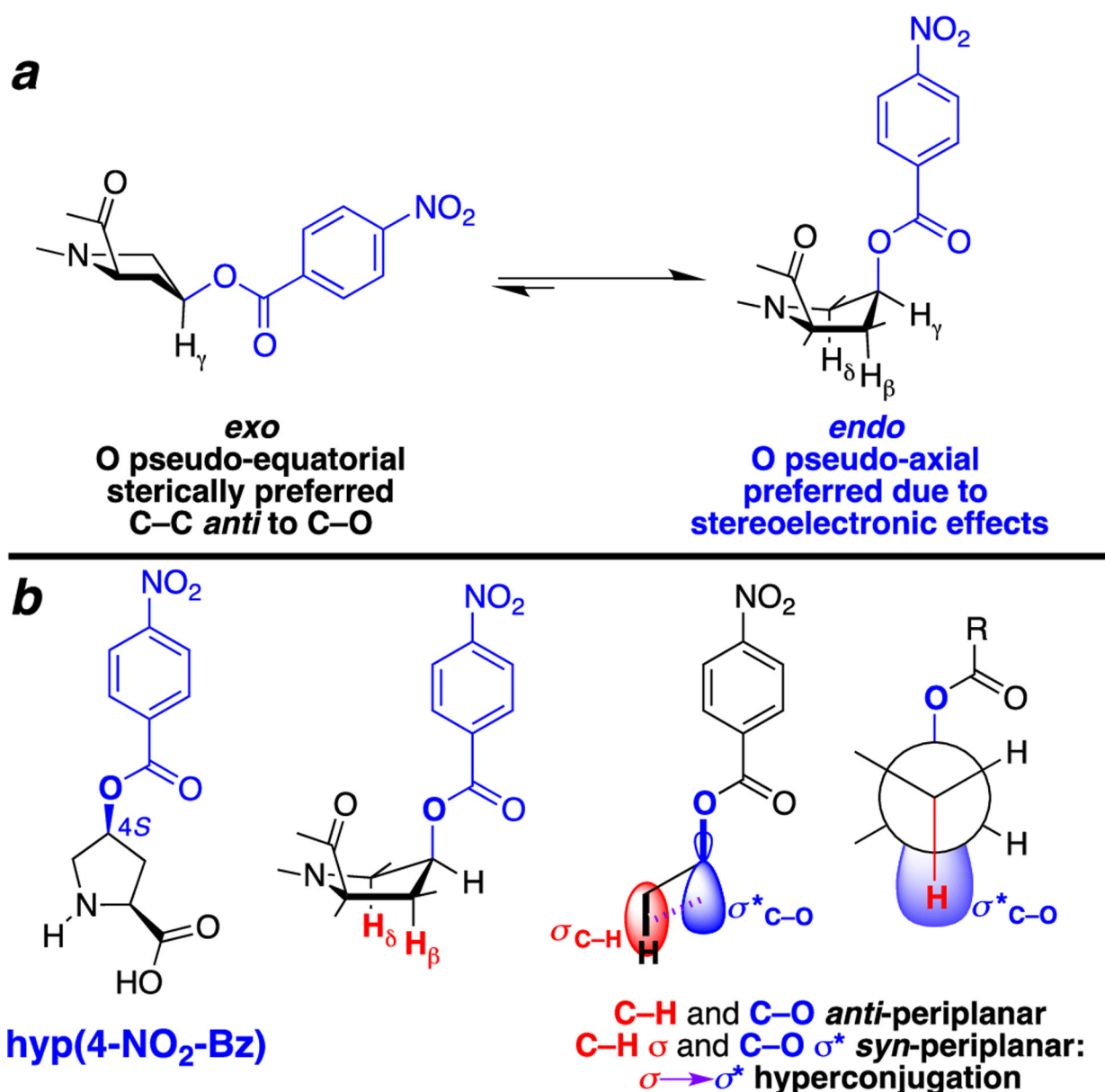
Author Manuscript

Author Manuscript

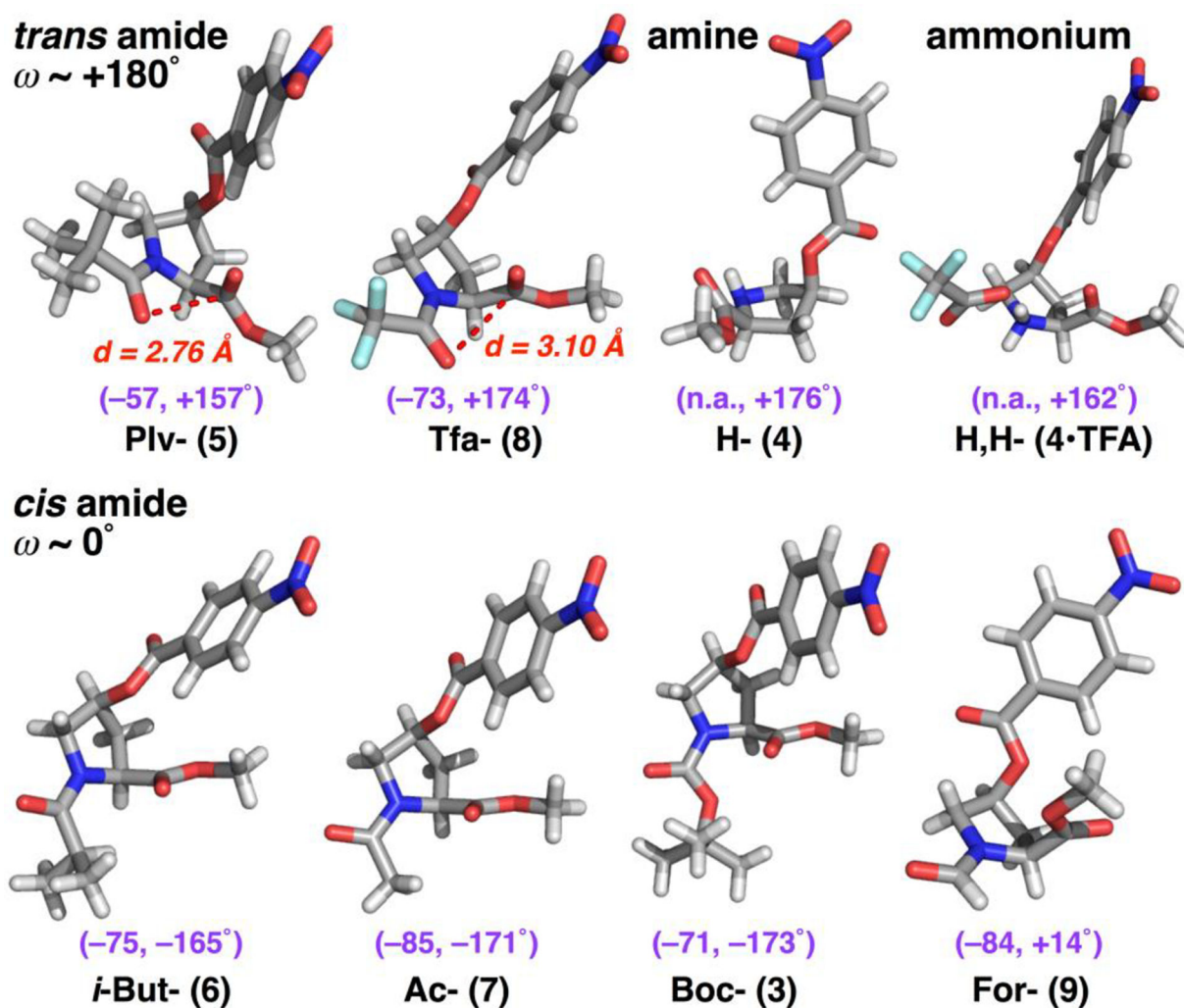
Author Manuscript

**Figure 1.**

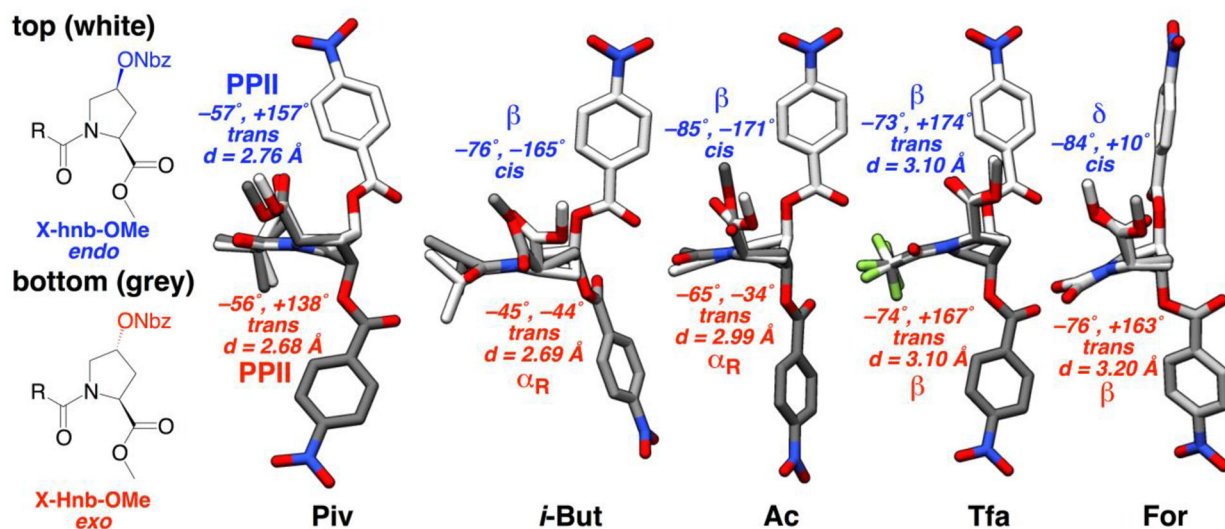
Proline conformational equilibria. (a) Proline *exo* and *endo* ring puckers. Puckering of proline at C $\gamma$  results in two envelope conformations of the pyrrolidine ring, the *exo* and *endo* ring puckers. Nomenclature is based on puckering of the  $\gamma$ -carbon toward (*endo*) or away from (*exo*) the carbonyl of the same residue. (b) Proline *trans* and *cis* amide conformations. Proline *cis*–*trans* isomerization has an activation barrier of  $\sim 20$  kcal mol $^{-1}$  (timescale of seconds to minutes at room temperature), whereas proline ring pucker interconversion has an activation barrier of 2–5 kcal mol $^{-1}$  (timescale of picoseconds at room temperature).<sup>[1c, 2]</sup>



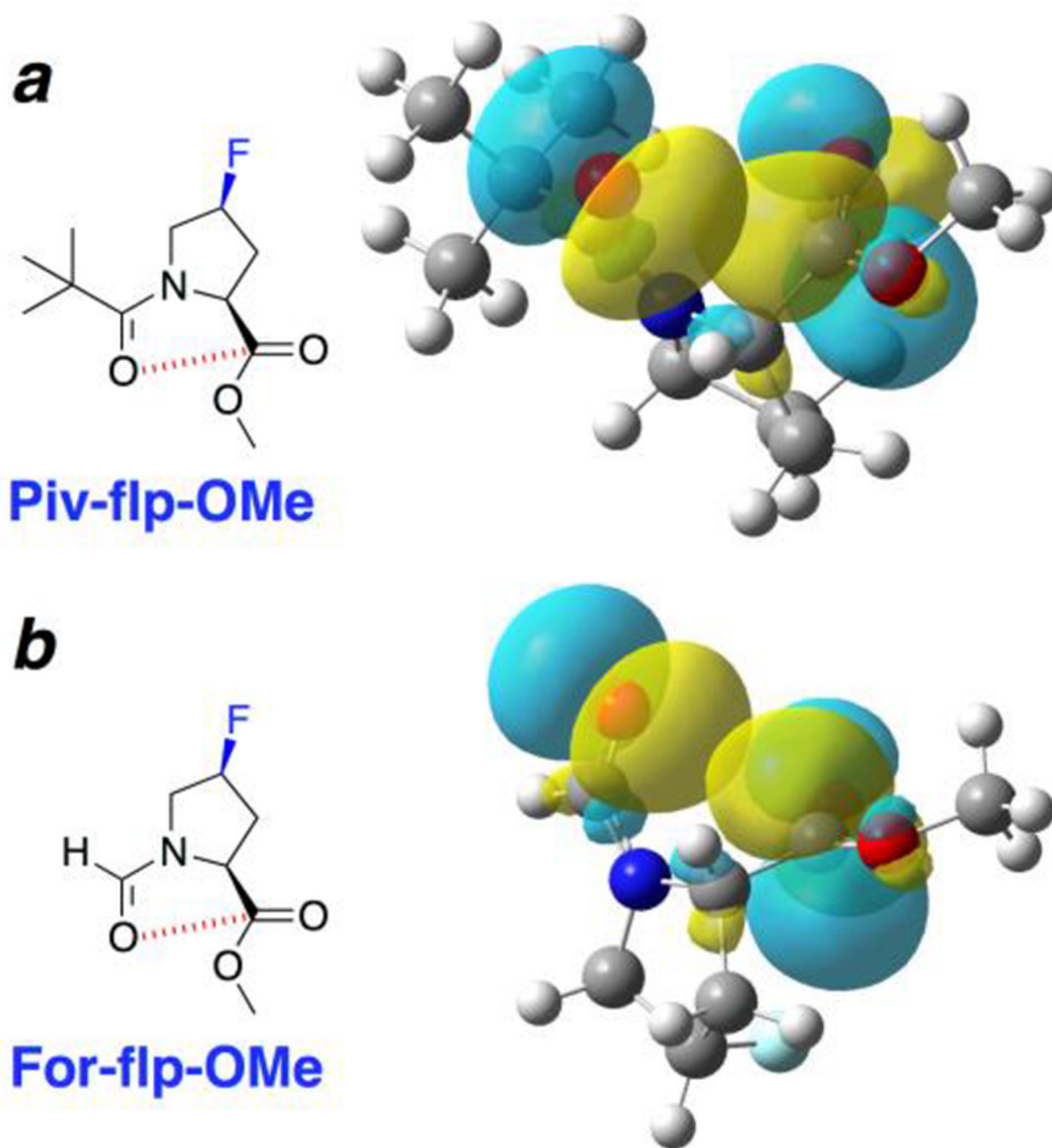
**Figure 2.** Side chain conformational preferences of 4*S*-hydroxyproline nitrobenzoate (hyp(4-NO<sub>2</sub>-Bz), hnb). (a) The nitrobenzoate preferentially adopts the sterically disfavored *endo* conformation, in which the nitrobenzoate is pseudo-axial on the pyrrolidine ring. (b) Hyperconjugative effects promote the *endo* ring pucker due to the presence of two C-H bonds (C-H $\beta$  and C-H $\delta$ ) *anti* to the nitrobenzoate. This conformation results in electron delocalization, via favorable orbital overlap between  $\sigma_{\text{C-H}}$  of the electron-rich C-H bonds and the  $\sigma^*$  antibonding orbital of the C-O bond. Localized depictions of key orbital lobes and limiting *gauche* conformations (CCCCO = 60° or HCCO = 180°) are shown. Observed HCCO torsion angles are typically 150–170° in 4*S*-substituted prolines (*vide infra* and ref. [6c]).



**Figure 3.** X-ray crystal structures of derivatives of 4*S*-hydroxyproline nitrobenzoate methyl ester.  $\phi$  and  $\psi$  torsion angles are indicated in magenta. Intercarbonyl distances ( $d$ ,  $O_j \dots C_{i+1}$ ) are indicated in red for molecules with *trans* amide bonds. All molecules exhibited an *endo* ring pucker crystallographically.

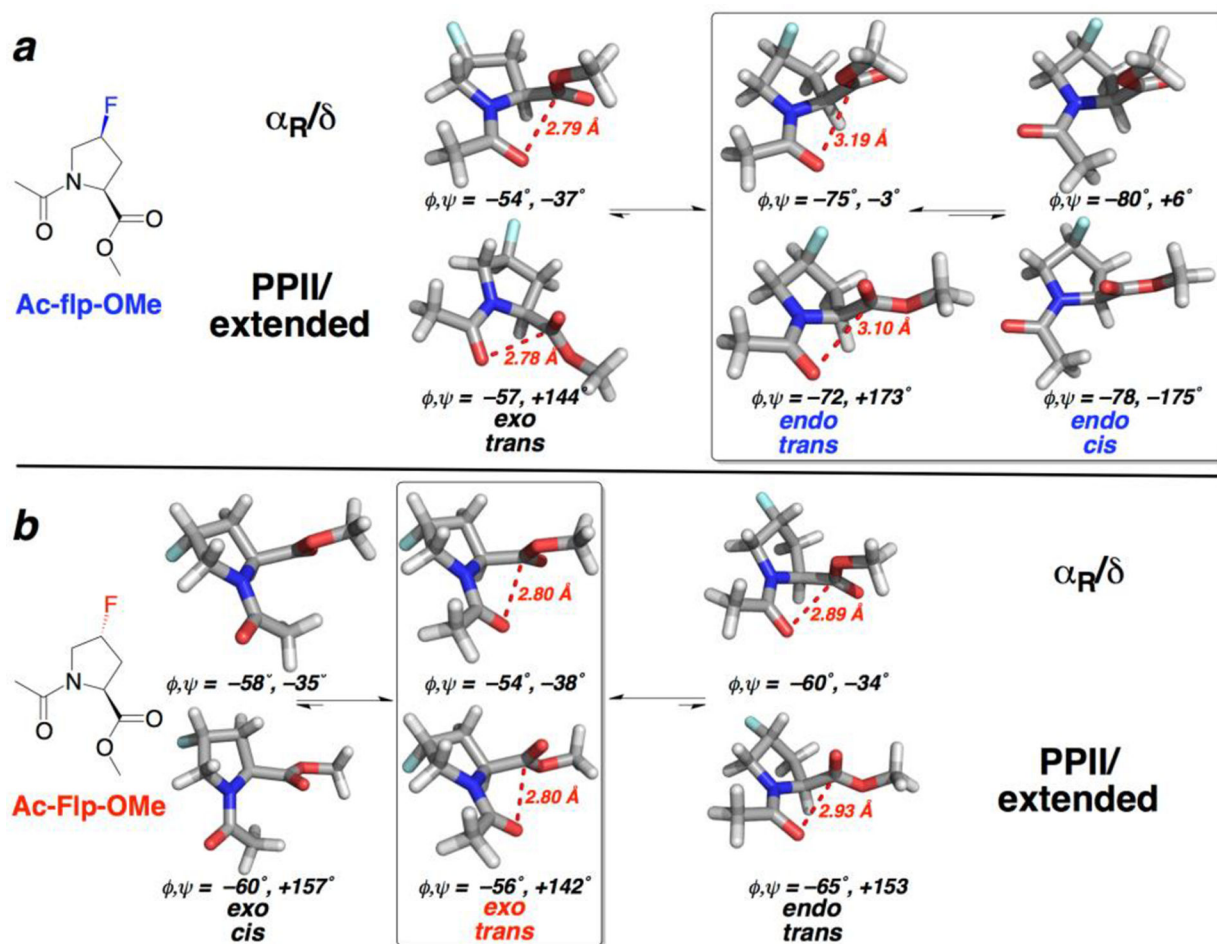
**Figure 4.**

Comparison of the structures of the 4*S*- (blue text, white carbons, top) and 4*R*- (red text, grey carbons, bottom) diastereomers of 4-hydroxyproline nitrobenzoate methyl esters, as a function of acyl N-capping group. Diastereomers were subjected to superposition of the N, C $\alpha$ , and C $\delta$  atoms using Chimera.<sup>[30]</sup> Nbz = 4-nitrobenzoyl.

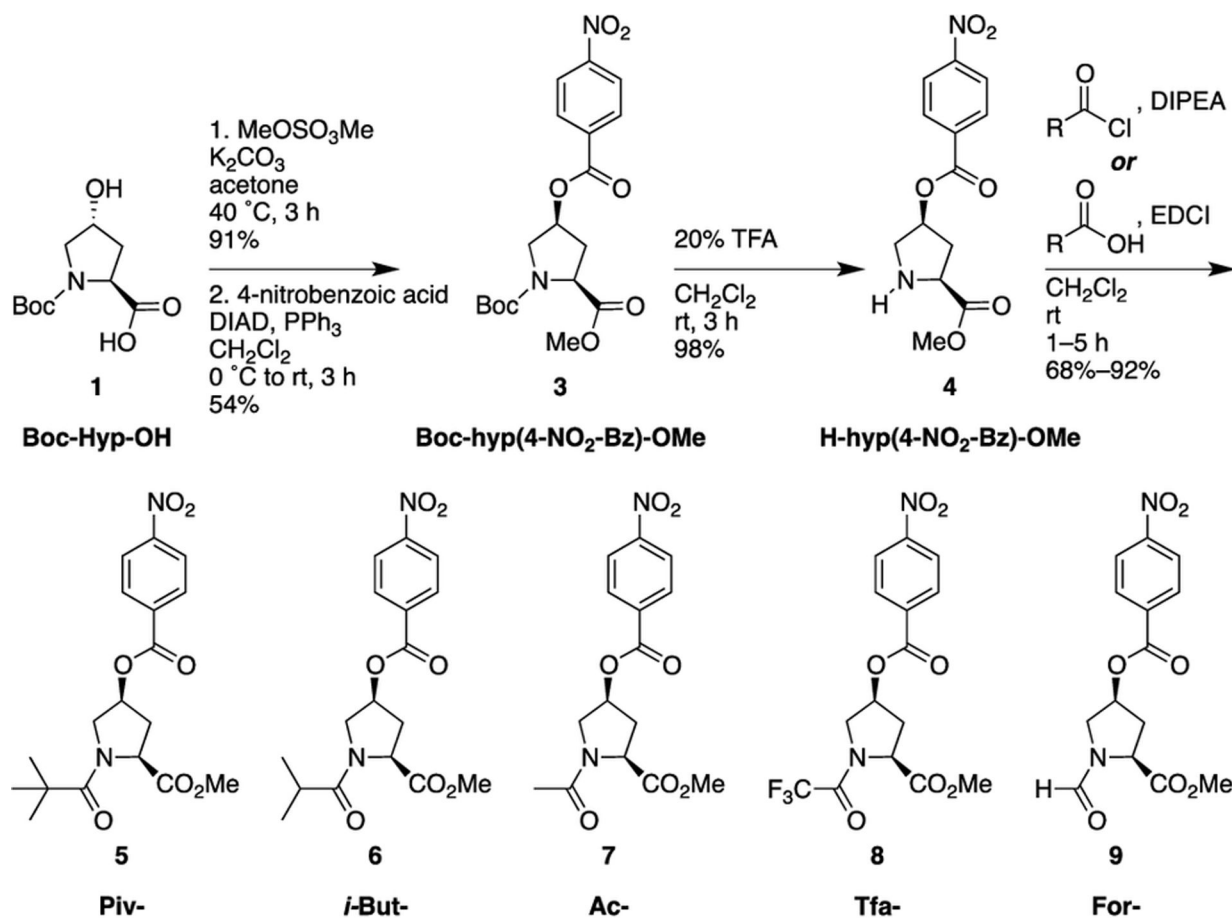


**Figure 5.** Natural bond orbital (NBO) analysis<sup>[25]</sup> of geometry-optimized structures of Piv-flp-OMe and For-flp-OMe, with a *trans* amide bond, *endo* ring pucker, and PPII/ $\beta$  conformation. By this analysis, the conformation in the pivaloyl derivative is stabilized by 0.52 kcal mol<sup>-1</sup> by the n $\rightarrow$  $\pi^*$  interaction, while in the formyl derivative the conformation is only stabilized by 0.12 kcal mol<sup>-1</sup>. These energy differences are reflected in the differing extents of orbital overlap and the divergent O<sub>*i*</sub>...C<sub>*i*+1</sub> intercarbonyl distances (Piv: d = 2.92 Å; For: d = 3.17 Å). Additional computational analysis as a function of acyl capping group and conformation is included in the Supporting Information.





**Figure 6.** Conformational landscape of 4*S*- and 4*R*-fluoroprolines as determined by computational investigations. Summary of computational results on (a) Ac-flp-OMe and (b) Ac-Flp-OMe. 4*S*-Fluoroproline (flp) (a, top) prefers an *endo* ring pucker, with both *trans* and *cis* amide bonds similar in energy. In contrast, 4*R*-fluoroproline (Flp) (b, bottom) prefers an *exo* ring pucker and a *trans* amide bond. Notably, for Ac-Flp-OMe, the *exo* ring is preferred in the *cis* amide conformation, while for Ac-flp-OMe the *endo* ring pucker typically observed for *cis*-proline is preferred, leading to substantially different preferred main chain conformations with either the *trans* or the *cis* amide conformation. Boxes indicate the lowest energy conformations for each diastereomer (conformations with energies within 0.6 kcal mol<sup>-1</sup> of the lowest energy conformation identified via DFT calculations). Conformations with energies > 2.8 kcal mol<sup>-1</sup> higher than the lowest energy conformation are not shown.

**Scheme 1.**Synthesis of 4*S*-hydroxyproline nitrobenzoate methyl ester derivatives.

**Table 1.**

Summary of the NMR data of the (2*S*,4*S*)-4-nitrobenzoyl-hydroxyproline methyl ester derivatives, with relative populations of *trans* and *cis* conformations determined via <sup>1</sup>H NMR spectroscopy in CDCl<sub>3</sub> at 298 K.

compound	X(C=O)-hyp(Nbz)-OCH <sub>3</sub> X=	$K_{\text{trans/cis}}^a$	$G_{\text{trans/cis}}^b$ , kcal mol <sup>-1</sup>
5	C(CH <sub>3</sub> ) <sub>3</sub> (Piv)	> 20 <sup>c</sup>	< -1.8
6	CH(CH <sub>3</sub> ) <sub>2</sub> ( <i>i</i> -But)	2.5	-0.54
7	CH <sub>3</sub> (Ac)	1.9	-0.38
8	CF <sub>3</sub> (Tfa)	2.8	-0.61
9	H (For)	0.7	+0.21
3	OC(CH <sub>3</sub> ) <sub>3</sub> (Boc)	0.8 <sup>d</sup>	+0.12

<sup>a</sup>  $K_{\text{trans/cis}}$  = ratio of the population of the species with *trans* amide bond to the population of the species with *cis* amide bond.

<sup>b</sup>  $G_{\text{trans/cis}} = -RT \ln K_{\text{trans/cis}}$ .

<sup>c</sup> Peaks corresponding to the *cis* isomer were not observed via <sup>1</sup>H NMR spectroscopy.

<sup>d</sup> Analysis of the H<sub>α</sub> and other chemical shifts is consistent with the *cis* isomer being the major species.

**Table 2.**

Summary of conformational data from crystal structures of 4*S*- and 4*R*- hydroxyproline nitrobenzoate methyl esters and other 4-substituted proline derivatives.<sup>a</sup>

4 <i>S</i> -substituted				4 <i>R</i> -substituted				
X-(C=O)- hyp(Nbz)-OMe	X-ray crystallography			X-(C=O)- Hyp(Nbz)-OMe <sup>b</sup>	X-ray crystallography			
X=	$\phi, \psi^\circ$	$\omega^\circ$	d, Å	X=	molecule 1		molecule 2	
					$\phi, \psi^\circ$	d, Å	$\phi, \psi^\circ$	d, Å
C(CH <sub>3</sub> ) <sub>3</sub> ( <b>5</b> ) (Piv)	-57, +157	+176	2.759	C(CH <sub>3</sub> ) <sub>3</sub> (Piv)	-56, +138	2.681	-	-
CH(CH <sub>3</sub> ) <sub>2</sub> ( <b>6</b> ) ( <i>i</i> -But)	-76, -165	+5	-	CH(CH <sub>3</sub> ) <sub>2</sub> ( <i>i</i> -But)	-45, -44	2.687	-47, -40	2.738
CH <sub>3</sub> ( <b>7</b> ) (Ac)	-85, -171	+10	-	CH <sub>3</sub> (Ac)	-65, -34	2.991	-69, -29	3.049
CF <sub>3</sub> ( <b>8</b> ) (Tfa)	-73, +174	-179	3.095	CF <sub>3</sub> (Tfa)	-74, +167	3.099	-	-
H ( <b>9</b> ) (For)	-84, +14	-1	-	H (For)	-76, +163	3.197	-84, +173	3.336
OC(CH <sub>3</sub> ) <sub>3</sub> ( <b>3</b> ) (Boc)	-71, -173	-7	-					
Fmoc-hyp(4-I-Ph)-OH <sup>c</sup>	-83, +177	+9	-					
Boc-hyp(4-I-Ph)-OH <sup>c</sup>	-76, +1	+1	-					
Boc-Hyp(4-I-Ph)-OMe <sup>c</sup>					-52, -39	2.836		
Ac-hyp-OMe <sup>d</sup>	-84, +18	0	-					
Ac-Hyp-OMe <sup>e</sup>					-51, +145	2.751	-63, +156	2.898
Ac-Hyp-OH <sup>f</sup>					-58, -32	2.832		
Boc-Hyp-OMe <sup>g</sup>					-55, -32	2.886		
Boc-hyp(Me)-OMe <sup>d</sup>	-85, +18	-1	-					
Ac-Hyp(Me)-OMe <sup>h</sup>					-58, +148	2.842		
Ac-Flp-OMe <sup>e</sup>					-55, +140	2.752	-56, +141	2.778

<sup>a</sup>Torsion angles and intercarbonyl distances were measured from the crystallographic structures. d = distance from O<sub>*j*</sub> to C<sub>*j+1*</sub>. hyp = (2*S*,4*S*)-hydroxyproline. Hyp = (2*S*,4*R*)-hydroxyproline. Nbz = nitrobenzoate ester. 4-I-Ph = 4-iodophenyl ether.

<sup>b</sup>Ref. [5b]. Most structures had two molecules in the unit cell; both structures are indicated in these cases.

<sup>c</sup>Ref. [20a], CSD[16] GABPAD, GABNUV, and GABPEH.

<sup>d</sup>Ref. [10b], CSD EMITEA and EMITIE.

<sup>e</sup>Ref. [20b], CSD RISDAY and RISDEC.

<sup>f</sup>Ref. [20c], CSD EXOBIE.

<sup>g</sup>Ref. [20d], CSD INEMIX.

<sup>h</sup>Ref. [12b], CSD SODJEB.

**Table 3.**

Summary of computational results on calculations on acetylated methyl esters of 4*S*-fluoroproline (flp) and 4*R*-fluoroproline (Flp).<sup>a</sup>

molecule	amide	pucker	quadrant	O...C=O			<i>E</i> <sub>rel</sub>
				d, Å	ϕ, °	ψ, °	kcal mol <sup>-1</sup>
Ac-flp-OMe	<i>trans</i>	<i>endo</i>	α <sub>p</sub> /δ	3.19	-75	-3	0.4
	<i>trans</i>	<i>endo</i>	PPII/β	3.10	-72	173	0.0
	<i>cis</i>	<i>endo</i>	α <sub>p</sub> /δ		-80	6	0.6
	<i>cis</i>	<i>endo</i>	PPII/β		-78	-175	0.2
	<i>trans</i>	<i>exo</i>	α <sub>p</sub> /δ	2.79	-54	-37	2.1
	<i>trans</i>	<i>exo</i>	PPII/β	2.78	-57	144	1.9
	<i>cis</i>	<i>exo</i>	α <sub>p</sub> /δ		-59	-34	3.7
	<i>cis</i>	<i>exo</i>	PPII/β		-61	158	3.3
Ac-Flp-OMe	<i>trans</i>	<i>exo</i>	α <sub>p</sub> /δ	2.79	-54	-38	0.2
	<i>trans</i>	<i>exo</i>	PPII/β	2.78	-56	142	0.0
	<i>cis</i>	<i>exo</i>	α <sub>p</sub> /δ		-58	-35	1.6
	<i>cis</i>	<i>exo</i>	PPII/β		-60	157	1.4
	<i>trans</i>	<i>endo</i>	α <sub>p</sub> /δ	2.89	-60	-34	2.4
	<i>trans</i>	<i>endo</i>	PPII/β	2.93	-65	153	1.9
	<i>cis</i>	<i>endo</i>	α <sub>p</sub> /δ		-72	-21	3.5
	<i>cis</i>	<i>endo</i>	PPII/β		-75	167	2.9

<sup>a</sup>Calculations were conducted at the DFT level of theory with the M06-2X method and the 6-311++G(3d,3p) basis set in implicit water. All structures are the result of geometry optimizations with the given combination of amide conformation (*trans* or *cis*), ring pucker (*exo* or *endo*), and quadrant of the Ramachandran plot (α-helix(α<sub>R</sub>)/δ conformation or PPII/extended(β) conformation). All energies are relative to the lowest energy conformation of the indicated diastereomer. All conformations within 0.6 kcal mol<sup>-1</sup> of the lowest energy conformation are indicated in color.